Science Advances
AAAS

advances.sciencemag.org/cgi/content/full/5/9/eaax6225/DC1

Supplementary Materials for

Discontinuous spread of millet agriculture in eastern Asia and prehistoric population dynamics

C. Leipe*, T. Long, E. A. Sergusheva, M. Wagner*, P. E. Tarasov

*Corresponding author. Email: c.leipe@fu-berlin.de (C.L.); mayke.wagner@dainst.de (M.W.)

Published 25 September 2019, *Sci. Adv.* **5**, eaax6225 (2019)
DOI: 10.1126/sciadv.aax6225

This PDF file includes:

Other Supplementary Material for this manuscript includes the following:

(available at advances.sciencemag.org/cgi/content/full/5/9/eaax6225/DC1)

Table S1 (Microsoft Excel format). Available ^{14}C dates directly derived from remains of domesticated millet extracted from the literature.
Table S2 (Microsoft Excel format). Newly obtained ^{14}C dates directly derived from remains of domesticated millet from prehistoric cultural layers in the Khanka-Ussuri region and the Chinese province of Shandong.

A

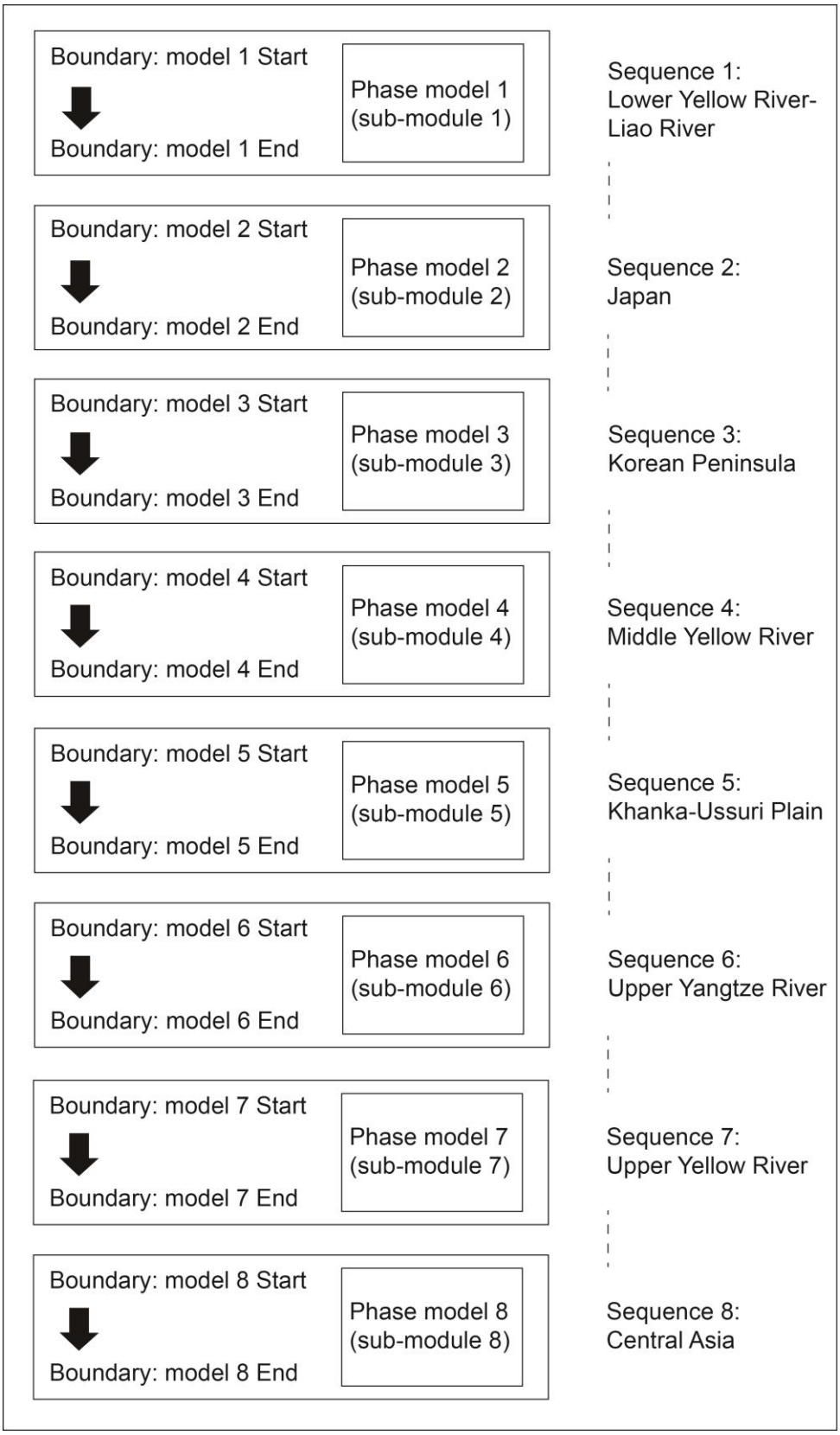
Boundary: model 1 Start
Boundary: model 1 End
Phase model 1 (sub-module 1)
Sequence 1: Lower Yellow River-Liao River
Boundary: model 2 Start
Boundary: model 2 End
Phase model 2 (sub-module 2)
Sequence 2: Japan
Boundary: model 3 Start
Boundary: model 3 End
Phase model 3 (sub-module 3)
Sequence 3: Korean Peninsula
Boundary: model 4 Start
Boundary: model 4 End
Phase model 4 (sub-module 4)
Sequence 4: Middle Yellow River
Boundary: model 5 Start
Boundary: model 5 End
Phase model 5 (sub-module 5)
Sequence 5: Khanka-Ussuri Plain
Boundary: model 6 Start
Boundary: model 6 End
Phase model 6 (sub-module 6)
Sequence 6: Upper Yangtze River
Boundary: model 7 Start
Boundary: model 7 End
Phase model 7 (sub-module 7)
Sequence 7: Upper Yellow River
Boundary: model 8 Start
Boundary: model 8 End
Phase model 8 (sub-module 8)
Sequence 8: Central Asia

B

```
Options()
 {
  kIterations=1000;
 };
 Plot()
 {
  Phase()
  {
   Sequence("Full_model_Lower_Yellow_River_Liao_River")
   {
    Boundary("Lower_Yellow_River_Liao_River_start",U(-9650,1950))
    {
     color="Red";
    };
    Phase("Lower_Yellow_River_Liao_River")
    {
     R_Date("BA-81608", 6900, 35);
     R_Date("Beta-456255", 6810, 30);
     R_Date("TO-12031", 6800, 35);
     R_Date("BA08804", 5550, 40);
     R_Date("BA08819", 5550, 35);
     R_Date("Beta-392668", 5390, 30);
     R_Date("BA08803", 5220, 35);
     R_Date("BA08805", 5195, 40);
     R_Date("Beta-325973", 4980, 40);
     R_Date("BK92065", 4950, 85);
     R_Date("Poz-47621", 4695, 35);
     R_Date("BA08811", 4690, 40);
     R_Date("Poz-47617", 4690, 35);
     R_Date("BA08809", 4685, 35);
     R_Date("Poz-47622", 4660, 35);
     R_Date("BA08807", 4655, 40);
```

R_Date("BA08815", 4645, 40);

R_Date("Poz-47625", 4640, 30);

R_Date("Poz-47623", 4570, 40);

R_Date("Poz-47618", 4555, 35);

R_Date("BA08814", 4535, 35);

R_Date("BA08816", 4530, 35);

R_Date("BA08818", 4505, 35);

R_Date("BA08810", 4480, 45);

R_Date("Poz-47619", 4470, 40);

R_Date("TO11417", 4330, 70);

R_Date("SNU04-537", 4260, 50);

R_Date("Beta-325971", 4160, 40);

R_Date("Poz-82357", 4015, 35);

R_Date("ZK-0415", 3990, 90);

R_Date("Poz-82355", 3965, 35);

R_Date("Beta-325968", 3910, 30);

R_Date("Beta-325964", 3870, 30);

R_Date("Poz-82373", 3825, 30);

R_Date("Beta-325173", 3800, 30);

R_Date("Poz-82353", 3765, 30);

R_Date("TO11418", 3740, 70);

R_Date("Beta-333381", 3710, 30);

R_Date("Poz-82364", 3690, 35);

R_Date("Poz-82361", 3655, 35);

R_Date("Beta-333383", 3650, 30);

R_Date("TO11419", 3600, 70);

R_Date("SNU04-986", 3590, 60);

R_Date("SNU05131", 3590, 40);

R_Date("SNU04-536", 3510, 40);

R_Date("BA06498", 3455, 55);

R_Date("Beta-394222", 3450, 30);

R_Date("BA06500", 3425, 35);

R_Date("BA06499", 3415, 35);

```
 R_Date("Beta-383366", 3360, 30);
 R_Date("Beta-382772", 3340, 30);
 R_Date("Beta-421461", 3280, 30);
 R_Date("Beta-334923", 3210, 30);
 R_Date("Poz-82366", 3105, 35);
 R_Date("SNU04-985", 3060, 50);
 R_Date("Beta-333386", 3030, 30);
 R_Date("Beta-333385", 2950, 30);
 R_Date("SNU04-538", 2940, 40);
 R_Date("BA081054", 2935, 35);
 R_Date("Beta-386787", 2880, 30);
 R_Date("Beta-394223", 2690, 30);
 R_Date("Beta-333382", 2540, 30);
 R_Date("Beta-392664", 2410, 30);
 R_Date("PV-0283", 2270, 80);
 R_Date("BK75005", 900, 85);
 };
 Boundary("Lower_Yellow_River_Liao_River_end",U(-9650,1950))
 {
  color="Red";
 };
};
Sequence("Full_model_Japan")
{
 Boundary("Japan_start",U(-9650,1950))
 {
  color="Red";
 };
 Phase("Japan")
 {
  R_Date("PLD-5304", 2550, 25);
  R_Date("?", 2530, 20);
  R_Date("PLD-5106", 2230, 20);
```

```
 R_Date("PLD-6466", 2185, 35);
 R_Date("TO-1998", 1160, 80);
 };
 Boundary("Japan_end",U(-9650,1950))
 {
  color="Red";
 };
};
Sequence("Full_model_Korean_Peninsula")
{
 Boundary("Korean_Peninsula_start",U(-9650,1950))
 {
  color="Red";
 };
 Phase("Korean_Peninsula")
 {
  R_Date("Beta-252973", 4770, 40);
  R_Date("TO8783", 4590, 100);
  R_Date("Beta-252972", 4340, 40);
  R_Date("TO8608", 4060, 140);
  R_Date("TO8607", 4030, 100);
  R_Date("UCIAMS67219", 3940, 20);
  R_Date("SNU07-543", 3090, 60);
  R_Date("TO8612", 2840, 60);
  R_Date("SNU-126", 2830, 60);
  R_Date("TO8637", 2800, 100);
 };
 Boundary("Korean_Peninsula_end",U(-9650,1950))
 {
  color="Red";
 };
};
Sequence("Full_model_Middle_Yellow_River")
```

```
{
 Boundary("Middle_Yellow_River_start",U(-9650,1950))
 {
  color="Red";
 };
 Phase("Middle_Yellow_River")
 {
  R_Date("Beta-425889", 5680, 30);
  R_Date("Beta-450597", 5350, 30);
  R_Date("BA130921", 4685, 30);
  R_Date("Beta-422852", 4410, 30);
  R_Date("BA130922", 4340, 30);
  R_Date("BA131926", 4305, 40);
  R_Date("BA130790", 4265, 25);
  R_Date("Beta-333389", 4180, 30);
  R_Date("Beta-411769", 4160, 30);
  R_Date("Beta-333387", 4150, 30);
  R_Date("Beta-465234", 4090, 30);
  R_Date("Beta-333388", 4070, 30);
  R_Date("BA131927", 3925, 25);
  R_Date("BA130789", 3820, 25);
  R_Date("BA130787", 3770, 30);
  R_Date("Beta-473868", 3760, 30);
  R_Date("Beta-486921", 3750, 30);
  R_Date("Beta-486923", 3730, 30);
  R_Date("Beta-486922", 3700, 30);
  R_Date("Beta-427728", 3680, 30);
  R_Date("BK84077", 3550, 90);
  R_Date("SA97030", 2900, 50);
  R_Date("ZK-5724", 2860, 33);
  R_Date("SA97029", 2850, 50);
 };
 Boundary("Middle_Yellow_River_end",U(-9650,1950))
```

```
 {
  color="Red";
 };
};
Sequence("Full_model_Khanka_Ussuri_Plain")
{
 Boundary("Khanka_Ussuri_Plain_start",U(-9650,1950))
 {
  color="Red";
 };
 Phase("Khanka_Ussuri_Plain")
 {
  R_Date("Poz-99460", 4130, 35);
  R_Date("Poz-99527", 3935, 30);
  R_Date("Poz-99525", 3925, 30);
  R_Date("Poz-99526", 3925, 30);
  R_Date("Poz-96977", 3885, 35);
  R_Date("TKa-14081", 3840, 35);
  R_Date("SNU04-192", 3090, 50);
  R_Date("TKa-13487", 3015, 50);
  R_Date("Poz-99459", 2945, 30);
  R_Date("Poz-99528", 2930, 30);
  R_Date("ZK-0085", 1650, 85);
  R_Date("TKa-13489", 1310, 45);
  R_Date("TKa-13488", 1310, 50);
 };
 Boundary("Khanka_Ussuri_Plain_end",U(-9650,1950))
 {
  color="Red";
 };
};
Sequence("Full_model_Upper_Yangtze_River")
{
```

```
Boundary("Upper_Yangtze_River_start",U(-9650,1950))
{
 color="Red";
};
Phase("Upper_Yangtze_River")
{
 R_Date("BA141207", 4520, 25);
 R_Date("BA141209", 4470, 25);
 R_Date("BA141211", 4470, 30);
 R_Date("BA141208", 4405, 35);
 R_Date("BA141210", 4240, 35);
 R_Date("BA120249", 4220, 35);
 R_Date("BA111228", 4115, 25);
 R_Date("SUERC- 73802", 4110, 34);
 R_Date("BA111229", 3995, 25);
 R_Date("Beta325960", 3980, 40);
 R_Date("SUERC-73806", 3929, 23);
 R_Date("BA111226", 3910, 25);
 R_Date("2010YMDT18-9-S1 ", 3665, 40);
 R_Date("BA081101", 3550, 40);
 R_Date("T1003-8-S2", 3275, 35);
 R_Date("T1003-9-S2", 3230, 40);
 R_Date("T1004-7-S3", 3210, 30);
 R_Date("T1004-6-S3", 3050, 30);
 R_Date("BA081100", 2940, 35);
 R_Date("T100454-S6", 2435, 30);
};
Boundary("Upper_Yangtze_River_end",U(-9650,1950))
{
 color="Red";
};
};
Sequence("Full_model_Upper_Yellow_River")
```

```
{
 Boundary("Upper_Yellow_River_start",U(-9650,1950))
 {
  color="Red";
 };
 Phase("Upper_Yellow_River")
 {
  R_Date("BA120182 ", 4530, 60);
  R_Date("TKa13889", 4490, 35);
  R_Date("BA120197", 4470, 25);
  R_Date("Beta-297655", 4410, 40);
  R_Date("BA110889", 4395, 40);
  R_Date("BA110899", 4370, 25);
  R_Date("Beta-292120", 4340, 41);
  R_Date("Beta-292119", 4340, 40);
  R_Date("Beta-292122", 4340, 40);
  R_Date("BA110882", 4300, 25);
  R_Date("BA110907", 4245, 30);
  R_Date("BA110909", 4185, 25);
  R_Date("BA110886", 4185, 35);
  R_Date("BA110908", 4135, 25);
  R_Date("ZK-0522", 4110, 95);
  R_Date("Beta-24458", 4110, 30);
  R_Date("BA120187", 4035, 30);
  R_Date("BA120201", 3980, 25);
  R_Date("BA120189", 3940, 25);
  R_Date("Beta-314721", 3900, 30);
  R_Date("BA110866", 3870, 30);
  R_Date("BA110906", 3840, 25);
  R_Date("OZK666", 3795, 50);
  R_Date("BA120202", 3755, 25);
  R_Date("OZM453", 3750, 35);
  R_Date("BA110912", 3715, 25);
```

```
 R_Date("BA110887", 3690, 30);
 R_Date("BA120204", 3680, 25);
 R_Date("BA110905", 3680, 25);
 R_Date("Beta-314717", 3640, 30);
 R_Date("Beta-303694", 3640, 30);
 R_Date("BA120217", 3630, 30);
 R_Date("BA110883", 3610, 20);
 R_Date("BA110879", 3600, 25);
 R_Date("BA110904", 3595, 25);
 R_Date("BA120199", 3410, 30);
 };
 Boundary("Upper_Yellow_River_end",U(-9650,1950))
 {
  color="Red";
 };
};
Sequence("Full_model_Central_Asia")
{
 Boundary("Central_Asia_start",U(-9650,1950))
 {
  color="Red";
 };
 Phase("Central_Asia")
 {
  R_Date("Beta-266458", 3840, 40);
  R_Date("BA05804", 3545, 40);
  R_Date("OS-92541", 3370, 25);
  R_Date("UBA-21939", 3330, 33);
  R_Date("BA05796", 3290, 40);
  R_Date("BA05793", 3240, 40);
  R_Date("BA05795", 3200, 40);
  R_Date("WB82-29", 3090, 90);
  R_Date("UBA-21941", 2091, 29);
```

```
    R_Date("UBA-21942", 2004, 29);
    R_Date("UBA-21945", 1844, 32);
   };
   Boundary("Central_Asia_end",U(-9650,1950))
   {
    color="Red";
   };
  };
 };
};
```

Fig. S1. Bayesian model structure and OxCal coding. (A) Bayesian model structure and (**B**) coding employed in OxCal v4.2.3 (https://c14.arch.ox.ac.uk/oxcal.html).

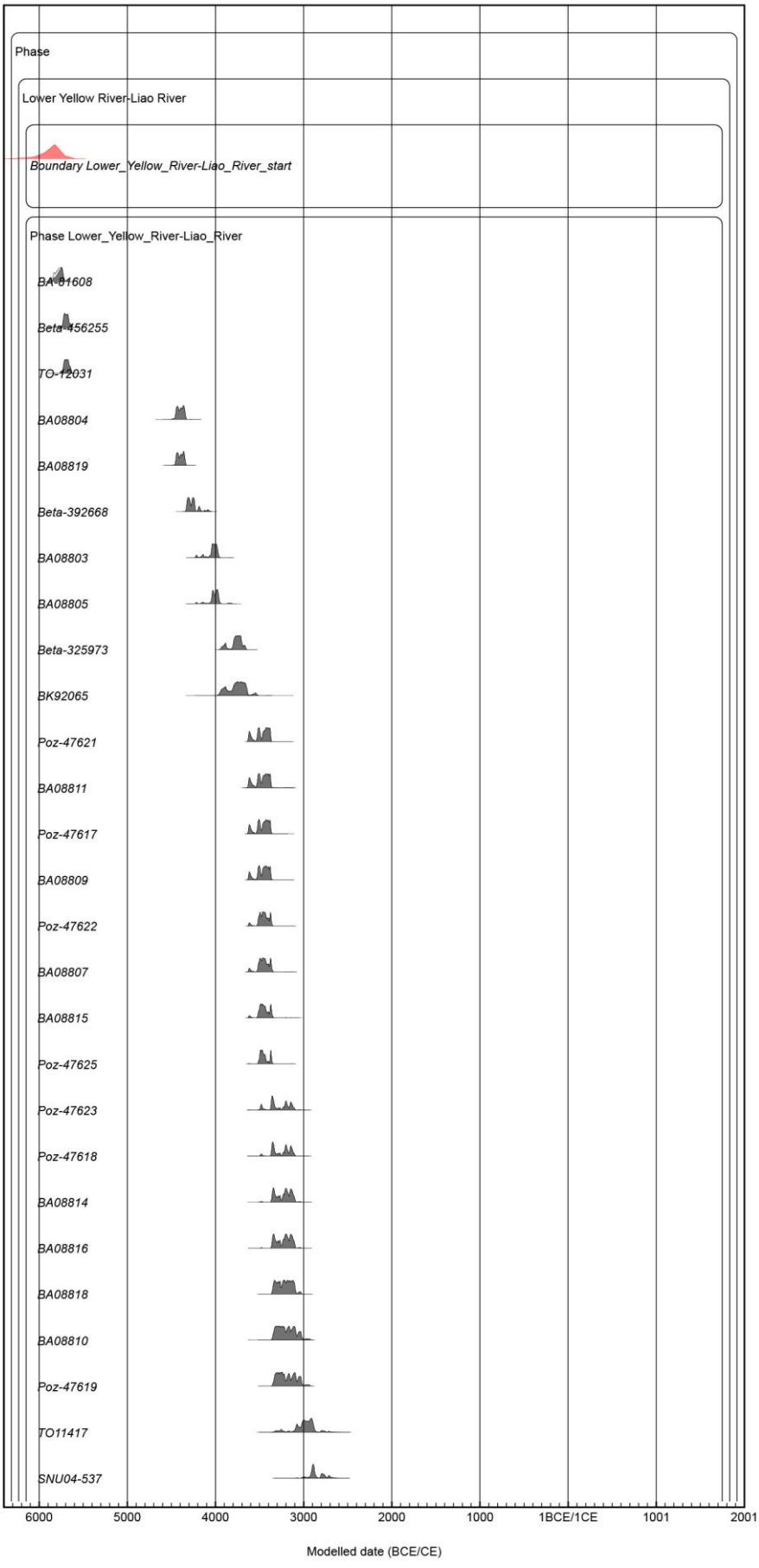
Phase
Lower Yellow River-Liao River
Boundary Lower_Yellow_River-Liao_River_start
Phase Lower_Yellow_River-Liao_River
BA81608
Beta-456255
TO-12031
BA08804
BA08819
Beta-392668
BA08803
BA08805
Beta-325973
BK92065
Poz-47621
BA08811
Poz-47617
BA08809
Poz-47622
BA08807
BA08815
Poz-47625
Poz-47623
Poz-47618
BA08814
BA08816
BA08818
BA08810
Poz-47619
TO11417
SNU04-537
6000
5000
4000
3000
2000
1000
1BCE/1CE
1001
2001
Modelled date (BCE/CE)

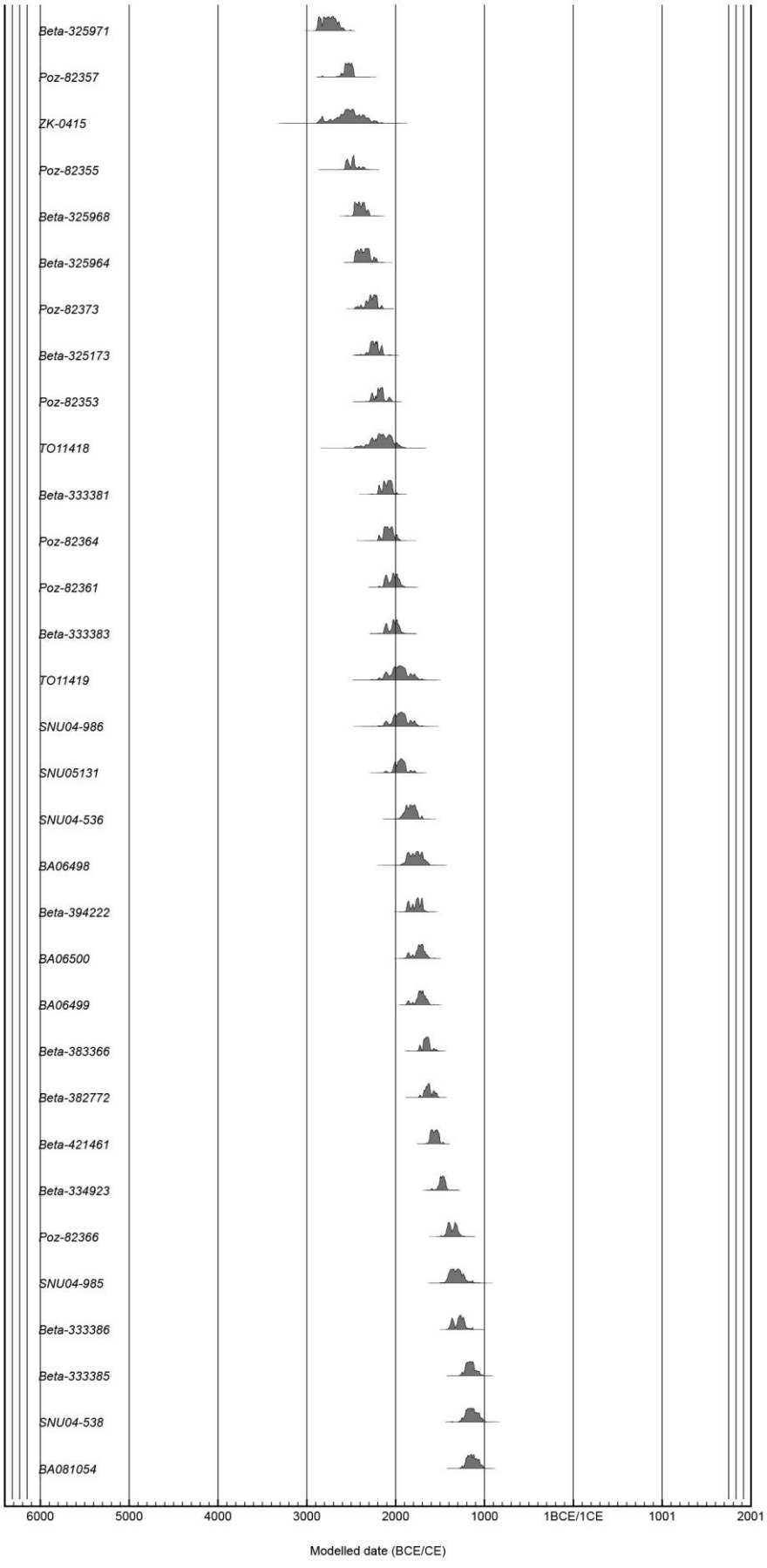
Beta-325971
Poz-82357
ZK-0415
Poz-82355
Beta-325968
Beta-325964
Poz-82373
Beta-325173
Poz-82353
TO11418
Beta-333381
Poz-82364
Poz-82361
Beta-333383
TO11419
SNU04-986
SNU05131
SNU04-536
BA06498
Beta-394222
BA06500
BA06499
Beta-383366
Beta-382772
Beta-421461
Beta-334923
Poz-82366
SNU04-985
Beta-333386
Beta-333385
SNU04-538
BA081054
6000
5000
4000
3000
2000
1000
1BCE/1CE
1001
2001
Modelled date (BCE/CE)

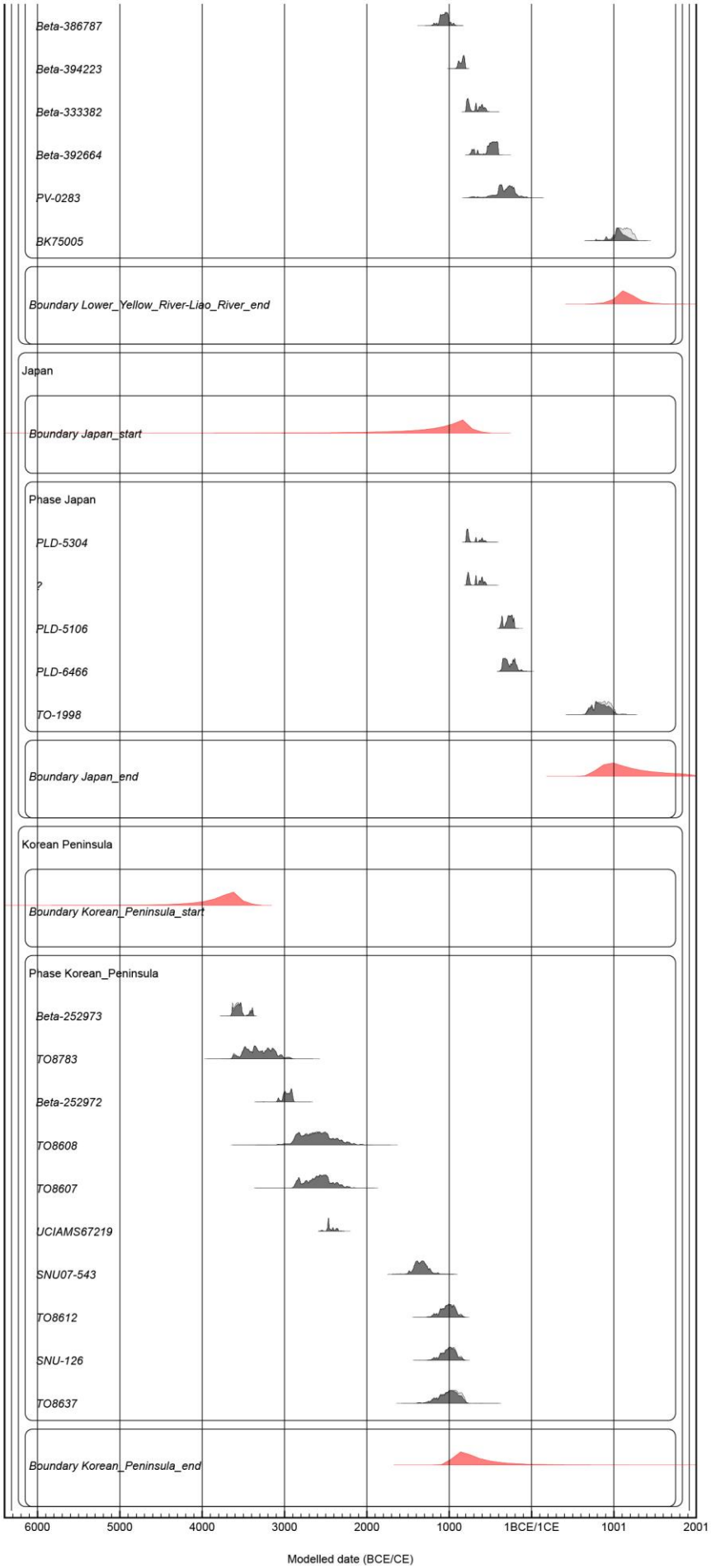
Beta-386787
Beta-394223
Beta-333382
Beta-392664
PV-0283
BK75005
Boundary Lower_Yellow_River-Liao_River_end
Japan
Boundary Japan_start
Phase Japan
PLD-5304
?
PLD-5106
PLD-6466
TO-1998
Boundary Japan_end
Korean Peninsula
Boundary Korean_Peninsula_start
Phase Korean_Peninsula
Beta-252973
TO8783
Beta-252972
TO8608
TO8607
UCIAMS67219
SNU07-543
TO8612
SNU-126
TO8637
Boundary Korean_Peninsula_end
6000
5000
4000
3000
2000
1000
1BCE/1CE
1001
2001
Modelled date (BCE/CE)

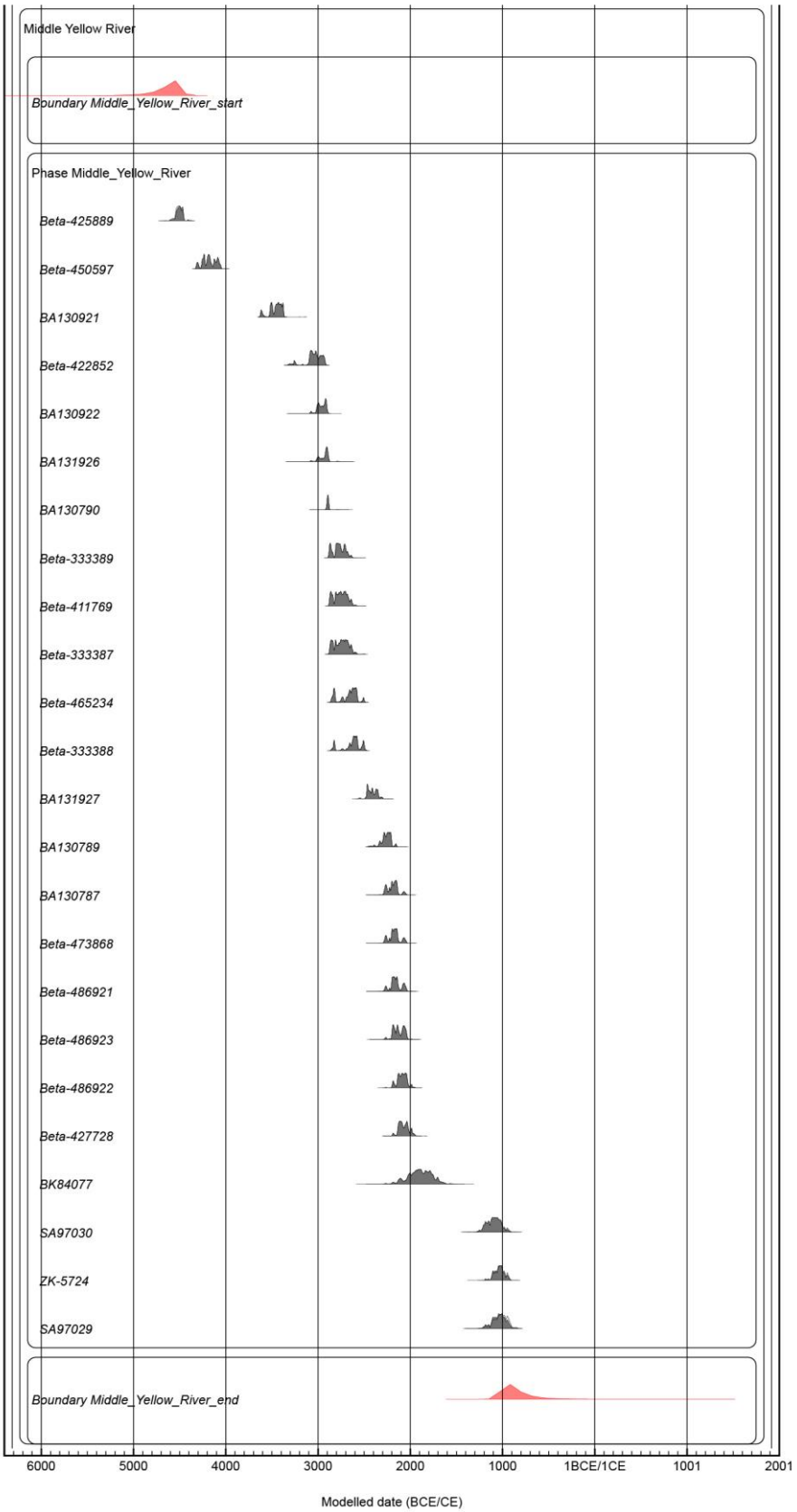
Middle Yellow River
Boundary Middle_Yellow_River_start
Phase Middle_Yellow_River
Beta-425889
Beta-450597
BA130921
Beta-422852
BA130922
BA131926
BA130790
Beta-333389
Beta-411769
Beta-333387
Beta-465234
Beta-333388
BA131927
BA130789
BA130787
Beta-473868
Beta-486921
Beta-486923
Beta-486922
Beta-427728
BK84077
SA97030
ZK-5724
SA97029
Boundary Middle_Yellow_River_end
6000
5000
4000
3000
2000
1000
1BCE/1CE
1001
2001
Modelled date (BCE/CE)

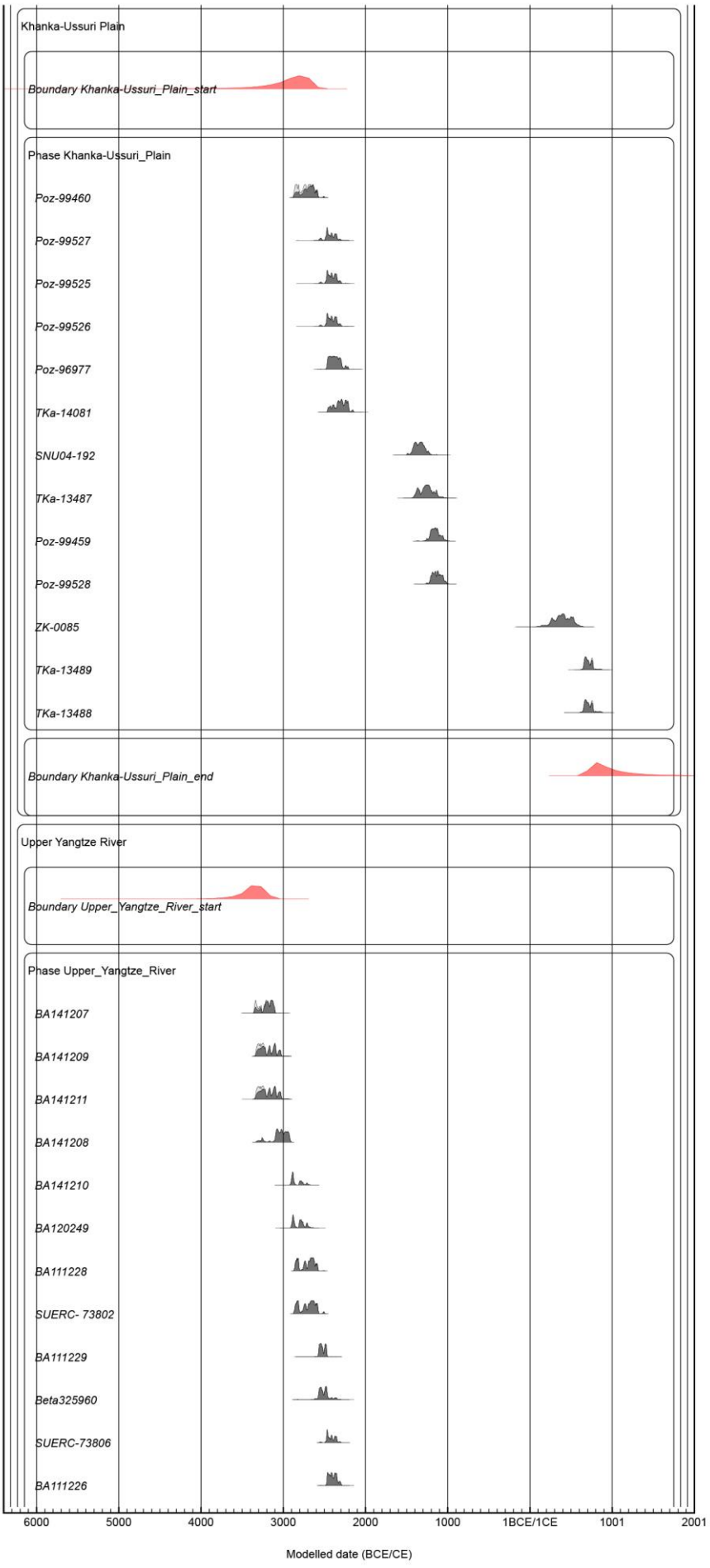
Khanka-Ussuri Plain
Boundary Khanka-Ussuri_Plain_start
Phase Khanka-Ussuri_Plain
Poz-99460
Poz-99527
Poz-99525
Poz-99526
Poz-96977
TKa-14081
SNU04-192
TKa-13487
Poz-99459
Poz-99528
ZK-0085
TKa-13489
TKa-13488
Boundary Khanka-Ussuri_Plain_end
Upper Yangtze River
Boundary Upper_Yangtze_River_start
Phase Upper_Yangtze_River
BA141207
BA141209
BA141211
BA141208
BA141210
BA120249
BA111228
SUERC- 73802
BA111229
Beta325960
SUERC-73806
BA111226
6000
5000
4000
3000
2000
1000
1BCE/1CE
1001
2001
Modelled date (BCE/CE)

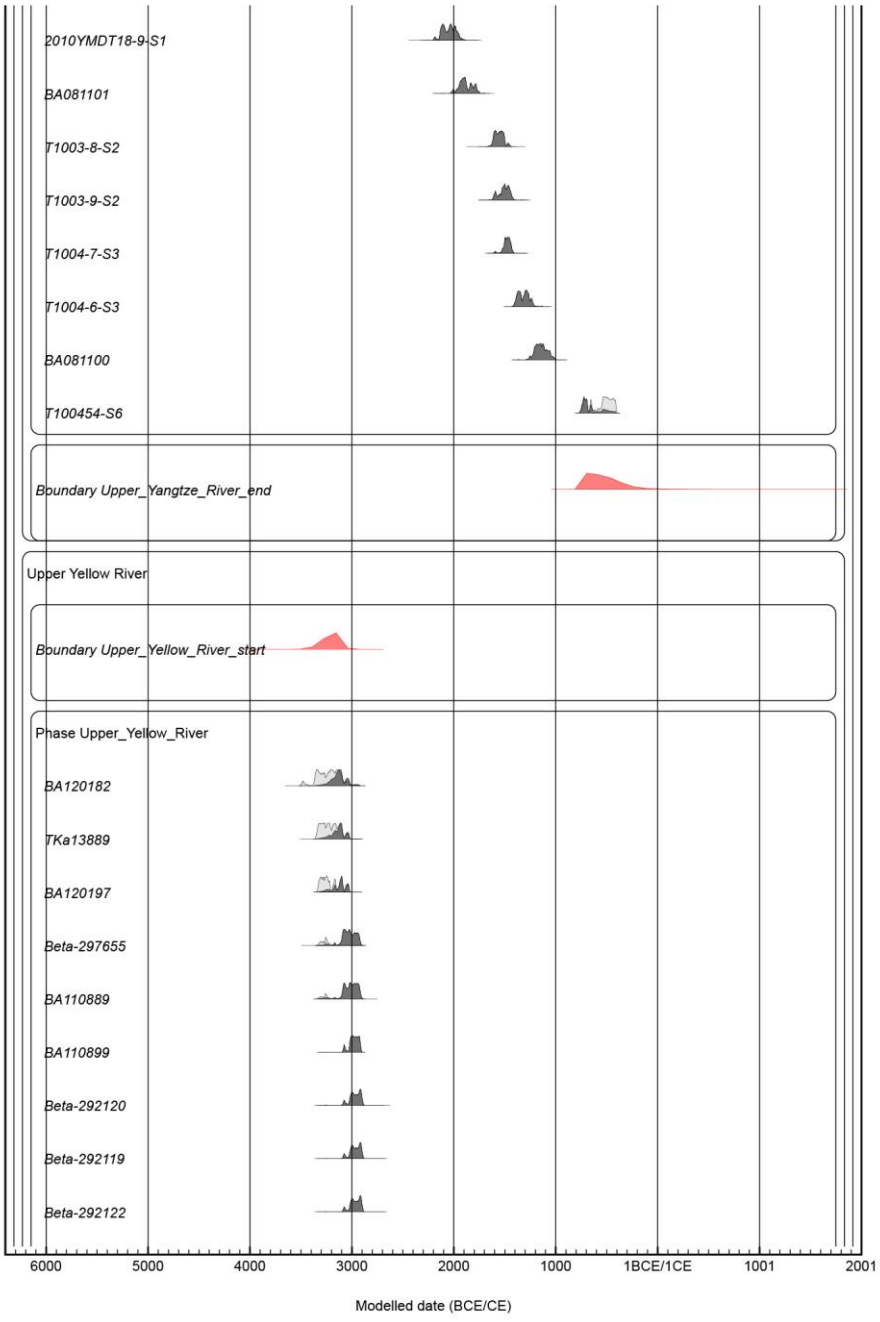
2010YMDT18-9-S1
BA081101
T1003-8-S2
T1003-9-S2
T1004-7-S3
T1004-6-S3
BA081100
T100454-S6
Boundary Upper_Yangtze_River_end
Upper Yellow River
Boundary Upper_Yellow_River_start
Phase Upper_Yellow_River
BA120182
TKa13889
BA120197
Beta-297655
BA110889
BA110899
Beta-292120
Beta-292119
Beta-292122
6000
5000
4000
3000
2000
1000
1BCE/1CE
1001
2001
Modelled date (BCE/CE)

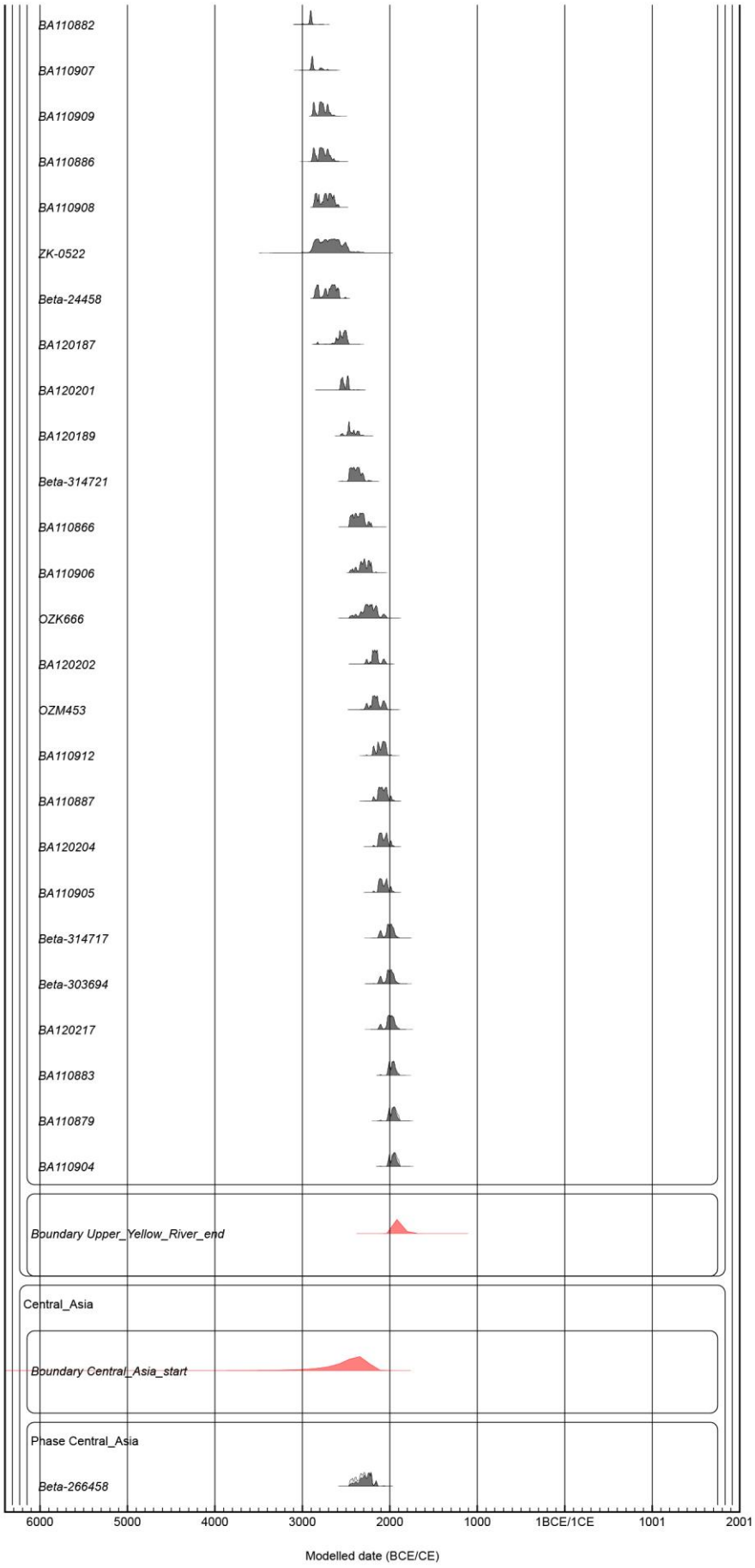
BA110882
BA110907
BA110909
BA110886
BA110908
ZK-0522
Beta-24458
BA120187
BA120201
BA120189
Beta-314721
BA110866
BA110906
OZK666
BA120202
OZM453
BA110912
BA110887
BA120204
BA110905
Beta-314717
Beta-303694
BA120217
BA110883
BA110879
BA110904
Boundary Upper_Yellow_River_end
Central_Asia
Boundary Central_Asia_start
Phase Central_Asia
Beta-266458
6000
5000
4000
3000
2000
1000
1BCE/1CE
1001
2001
Modelled date (BCE/CE)

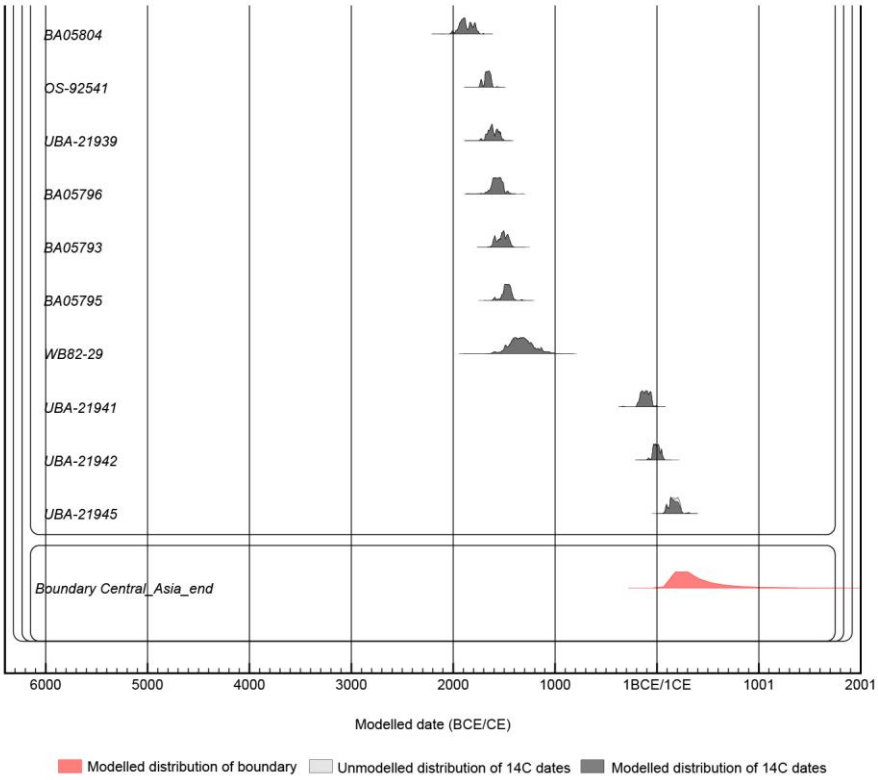

Fig. S2. OxCal modeling results. The results of Bayesian modelling applied to the compiled set of published (table S1) and newly (table S2) obtained millet ^{14}C dates (n = 184). Light grey and dark grey silhouettes represent unmodelled and modelled 95% probability distribution of ^{14}C dates, respectively. Red silhouettes represent the modelled probability distribution of the boundaries.